VIP Enzyme Models

DOI: 10.1002/anie.200904572

Spectroscopic Characterization of a Hydroperoxo–Heme Intermediate: Conversion of a Side-On Peroxo to an End-On Hydroperoxo Complex**

*Jin-Gang Liu, Takehiro Ohta, Satoru Yamaguchi, Takashi Ogura, Satoshi Sakamoto, Yonezo Maeda, and Yoshinori Naruta**

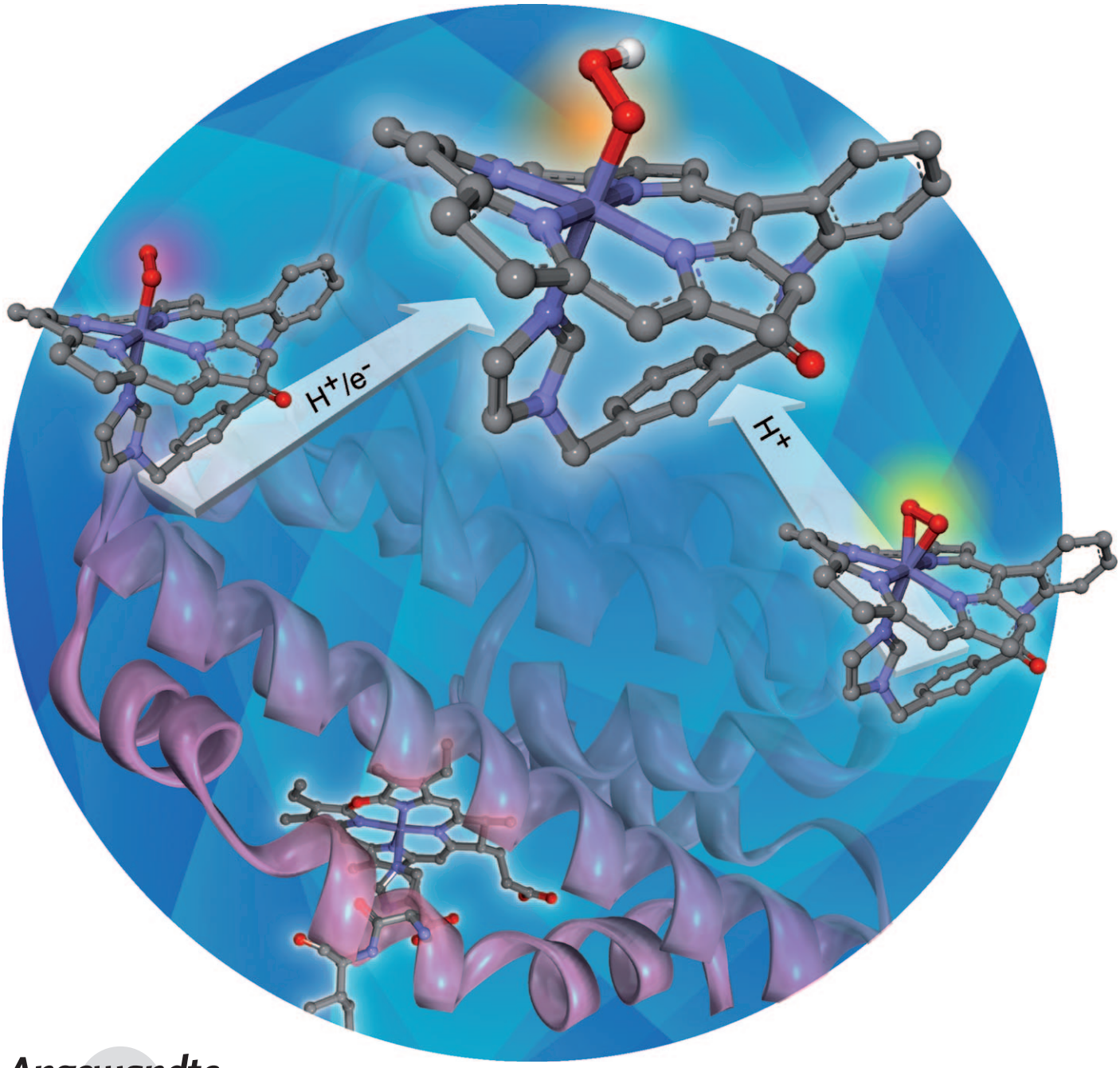

The ferric hydroperoxo–heme species [Fe–OOH] (compound 0) is well known as a common key intermediate in the catalytic cycles of heme-containing monooxygenase and peroxidase enzymes.[1–4] The catalytic cycles of nitric oxide synthase,[1] cytochrome P450,[2] and heme oxygenase (HO)[3] generally involve single-electron reduction of an oxy–ferrous intermediate to form a ferric peroxo species. This process is often coupled with proton transfer to the distal oxygen atom of the peroxo intermediate to afford the ferric hydroperoxo species. The ferric hydroperoxo–heme species has also been suggested to be a plausible intermediate in the catalytic cycle of cytochrome *c* oxidase (C*c*O).[5] Although the crucial role of ferric (hydro)peroxo hemes has been widely recognized, the transient character of these intermediates has hampered efforts to characterize them during catalytic turnover under physiological conditions. The generation of ferric (hydro)-peroxo intermediates in heme enzymes is typically achieved by radiolytic reduction of the corresponding ferrous–oxy [$Fe^{III}(O_2^-)$] precursor at cryogenic temperature (77 K).[6–9]

Owing to their relevance to enzymatic transformations, (hydro)peroxo porphyrin model complexes have been actively investigated.[5,10–14] The frequently observed intermediates are high-spin side-on peroxo species,[11,12] and the infrequently reported low-spin hydroperoxo models, which are mainly observed by UV/Vis and EPR spectroscopy, are ligated by an exogenous axial ligand.[13] Characterization of such low-spin (hydro)peroxo–heme complexes by resonance Raman spectroscopy (rR) has not yet been reported. In our previous synthetic model studies of C*c*O, we reported a series of copper-ion-bridged heme peroxides.[14] Herein, we describe efficient methods for the preparation of a low-spin end-on ferric hydroperoxo heme species [(tmpIm)Fe^{III}–OOH] (**2**, Scheme 1) that possesses a covalently linked axial imidazole (Im) ligand, as confirmed by UV/Vis, EPR, rR, and Mössbauer spectroscopy. Our experimental results demonstrate that protonation of a side-on high-spin heme peroxide leads to the formation of the corresponding end-on low-spin hydroperoxide. This reaction represents the first example of a spin-state and binding-mode switch of heme peroxide that is triggered by protonation.

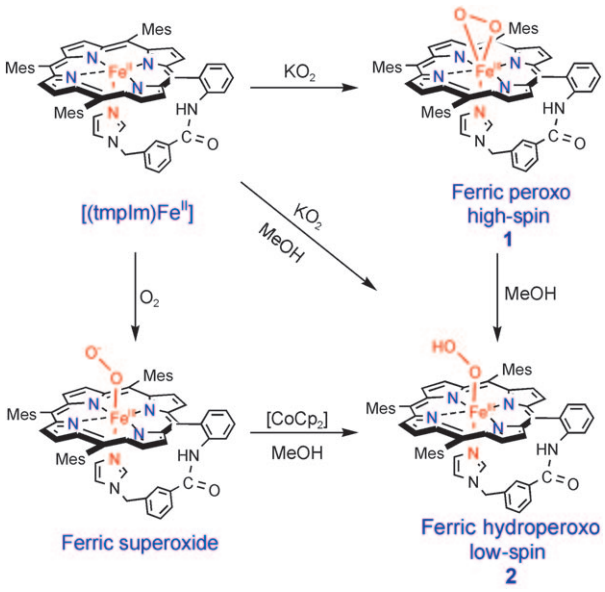

Scheme 1. Selective preparation of hydroperoxo–heme species **2** by different routes.

The model compound [(tmpIm)Fe^{II}] was prepared according to a procedure similar to the multistep method described in our previous report[14a] starting from 5,10,15-trismesityl-20-(2-nitrophenyl)porphyrin. In the next step, a solution of [(tmpIm)Fe^{II}] in MeCN/THF (20:80) at −30 °C reacted rapidly with KO_2, which was solubilized with [2,2,2]cryptand in MeCN, to afford a brownish-green complex **1**. This complex has a UV/Vis spectrum ($(\lambda_{max}$ (ε/$M^{-1}cm^{-1}$) = 440 (1.1×10^5), 574 (1.1×10^4), 615 nm (7.0×10^3); Figure 1) that is similar to that of a side-on peroxo species [(tmp)$Fe^{III}(O_2^{2-})$] (tmp = 5,10,15,20-tetrakis(2,4,6-trimethylphenyl)porphyrin; λ_{max}(ε/$M^{-1}cm^{-1}$) = 439 (1.3×10^5), 569 (1.2×10^4), 614 nm ($6.5\times$

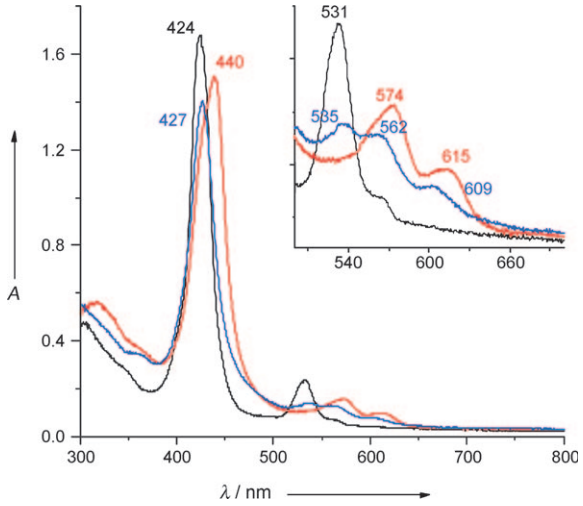

Figure 1. UV/Vis spectra of [(tmpIm)Fe^{II}] (black trace), and its reaction with KO_2 to afford complex **1** (red trace) in MeCN/THF (20:80) at −30 °C. Protonation of complex **1** by methanol yields complex **2** (blue trace) at −65 °C. The inset shows the magnified Q-band region.

[*] Dr. J.-G. Liu, Dr. T. Ohta, Prof. Dr. Y. Naruta
Institute for Materials Chemistry and Engineering
Kyushu University
Higashi-ku, Fukuoka, 812-8581 (Japan)
Fax: (+81) 92-642-2715
E-mail: naruta@ms.ifoc.kyushu-u.ac.jp
Homepage: http//narutalab.ifoc.kyushu-u.ac.jp
S. Sakamoto, Prof. Dr. Y. Maeda
Graduate School of Sciences, Kyushu University
Higashi-ku, Fukuoka 812-8581 (Japan)
Dr. S. Yamaguchi, Prof. Dr. T. Ogura
Graduate School of Life Sciences, University of Hyogo
Hyogo, 678-1297 (Japan)

[**] This work was financially supported by Grants-in-Aid for Scientific Research (S) (no. 17105003, YN), for Young Scientists (B) (no. 27150173, JGL) from JSPS, on Priority Areas (no. 19027044, YN), Innovative Areas (no. 20200050, JGL) from MEXT; and by the Elemental Science and Technology Project from MEXT. The 430 nm laser was set up by Dr. Ken'ichi Nakagawa, The University of Electro-Communications (Japan).

Supporting information for this article is available on the WWW under http://dx.doi.org/10.1002/anie.200904572.

10^3)) prepared under similar experimental conditions (Figure S1 in the Supporting Information). The EPR spectrum of complex **1** (Figure 3a) has a typical rhombic marker signal at $g \approx 4.2$, which is similar to that of [(tmp)$Fe^{III}(O_2^{2-})$] and is consistent with a η^2-peroxo–heme species. Complex **1** was then further characterized by rR spectroscopy. The rR spectra of complex **1** show two groups of isotope shifts (Figure 2). One band appears at 807 cm^{-1} and shifts to 758 cm^{-1} upon ^{18}O substitution. This band is assignable to the ν(O–O) stretching vibration of a peroxo species. The other band at 475 cm^{-1} (^{16}O) and 455 cm^{-1} (^{18}O) is assigned to the ν(Fe–O) stretching vibration. The relatively lower frequency of ν(Fe–O) is similar to that of the nonheme η^2-peroxo complexes.[15] For comparison, the ν(O–O) and ν(Fe–O) stretching vibrations of the side-on compound [(tmp)$Fe^{III}(O_2^{2-})$] appear at 809 cm^{-1} and 470 cm^{-1}, respectively (Figure S2 in the Supporting Information). These results suggest that, for compound **1**, the ν(O–O) stretching is 2 cm^{-1} lower and ν(Fe–O) is 5 cm^{-1} higher than that of the imidazole-free side-on peroxo [(tmp)$Fe^{III}(O_2^{2-})$]. This result may be an indication that binding of the axial imidazole ligand to iron weakens the O–O bond by increasing the π*-orbital electron density. The Fe–O bond is strengthened by back-donation from the oxygen to the iron atom and by electron donation of the imidazole ligand to the oxygen π* orbital through the trans effect. The implication of association of the imidazole with the iron porphyrin is further supported by the following observation: in the presence of the coordinating solvent DMSO, the side-on peroxo compound [(dmso)(tmp)$Fe^{III}(O_2^{2-})$] exhibited dramatically increased nucleophilicity relative to the parent compound [(tmp)$Fe^{III}(O_2^{2-})$], as a result of the axial association of DMSO to the iron porphyrin.[12c–d] The rR spectrum of [(dmso)(tmp)$Fe^{III}(O_2^{2-})$] has ν(O–O) and ν(Fe–O) bands at 807 cm^{-1} and 476 cm^{-1}, respectively (Figure S3 in the Supporting Information). These bands are essentially the same as those of complex **1**. The observed ν(O–O) value is comparable to that of similar side-on heme peroxide obtained by IR spectroscopy.[12f] These results may suggest that complex **1** is a seven-coordinate (7c) side-on peroxide species. To the best of our knowledge, this is the first reliable rR evidence for this type of side-on heme peroxides.[12f]

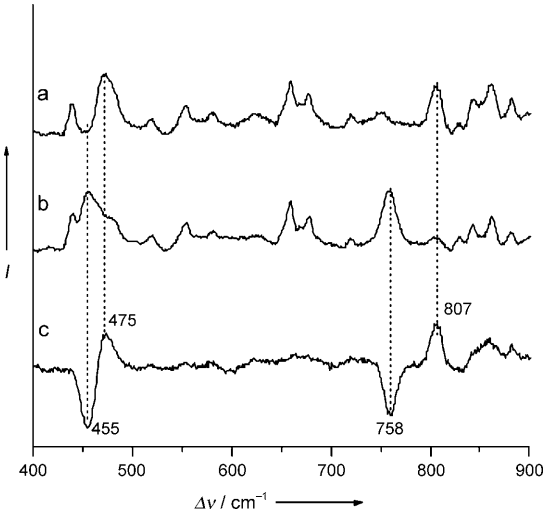

Figure 2. Resonance Raman spectra of complex **1** containing a) ^{16}O and b) ^{18}O. c) Difference spectrum of (a)–(b). $\lambda_{ex} = 441.6$ nm, 77 K.

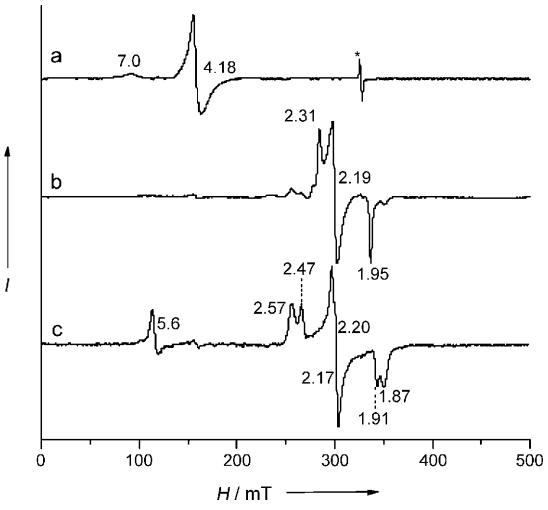

Figure 3. EPR spectra of a) complex **1**, b) **2**, and c) the room-temperature decomposition product of **2**, 77 K. The signal labeled with an asterisk originates from residual O_2^- in the solution.

The most striking difference between complex **1** and [(tmp)$Fe^{III}(O_2^{2-})$], (7c versus 6c side-on peroxo), comes from their reactivity toward protonation. Addition of methanol (400 equivalents) to a solution of complex **1** in MeCN/THF (20:80) at −65 °C afforded a new species, complex **2**. The electronic absorption spectrum of complex **1** underwent distinct spectral changes upon addition of methanol, with a shift in the Soret band from 440 nm to 428 nm and a split in the Q bands to 535, 562, and 609 nm (Figure 1). The UV/Vis features are similar to those of the previously reported hydroperoxo–heme model compounds such as [(tmp)Fe^{III}-(−OH)(−OOH)] ($\lambda_{max} = 428$, 563, 601 nm).[13a] The EPR experiments further confirmed this transformation. Protonation of complex **1** caused the disappearance of the signal at $g \approx 4.2$ and a new set of signals appeared at $g = 2.31$, 2.19, and 1.95 (Figure 3b). This result clearly indicates the signature of a low-spin ferric heme species in a strong field with small *g* dispersion. This set of *g* values corresponds very well with those of the previously reported hydroperoxo–heme model compound [(Im)(tmp)Fe^{III}(−OOH)] ($g = 2.32$, 2.19, 1.94),[13a] and is similar to the *g* values of the end-on ferric hydroperoxo–heme intermediate generated in enzymes using cryoradiolytic methods. For example, the *g* values of the ferric hydroperoxo–heme intermediate of hemoglobin are 2.31, 2.18, and 1.94.[6] The formation of MeOH/MeO^--bound low-spin ferric species is ruled out by these observed *g* values, as can be seen from the EPR spectrum of the room-temperature decomposed product, which shows a wide span of *g* values (Figure 3c). On the other hand, for the six-coordinate (6c) side-on peroxide [(tmp)$Fe^{III}(O_2^{2-})$], protonation under similar experimental conditions produces no new intermediates and leads directly to decomposition of the peroxide (Figure S4 in the Supporting Information). Thus, protonation of a 7c side-on peroxide switches the closed form to an end-on hydroperoxide. These results indicate that axial

imidazole ligation to the heme iron is crucial for the generation of the hydroperoxo species.

Preparation of the hydroperoxo species could also be achieved by reaction of [Fe^{II}(tmpIm)] with KO_2 in the presence of methanol at −75 °C. Upon addition of KO_2 to a EtCN/THF (20:80) solution of [Fe^{II}(tmpIm)] containing methanol (400 equiv), the Soret band immediately shifted from 423 nm ($\varepsilon = 1.1 \times 10^5$) to 427 nm ($9.9 \times 10^4$) and the Q bands shifted from 532 (1.6×10^4), 564 (8.6×10^3) to 533 (1.2×10^4), 564 (1.0×10^4), and 609 nm (7.3×10^3; Figure 4).

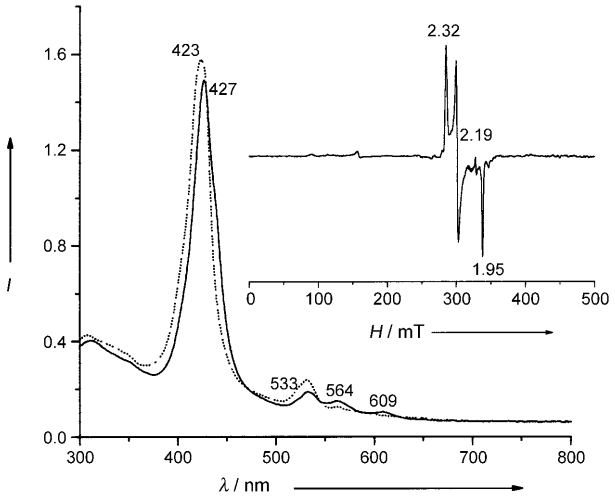

Figure 4. UV/Vis spectra of complex **2** (——) prepared from reaction of KO_2 with [(tmpIm)Fe^{II}] (•••••) in the presence of methanol (400 equiv) in EtCN/THF (20:80) at −75 °C. The inset shows the EPR spectrum of complex **2** prepared as described above.

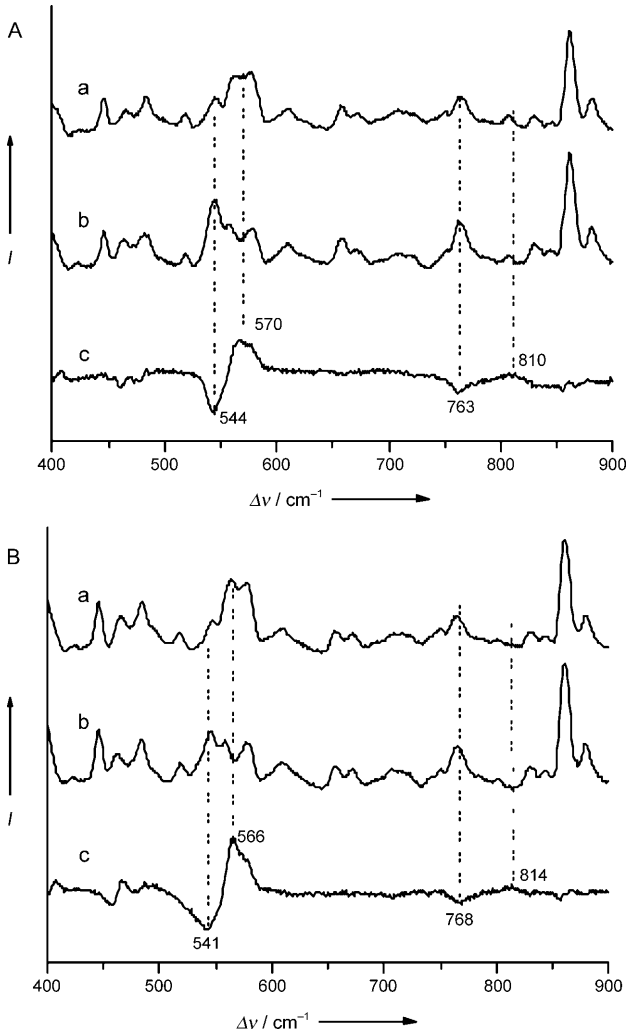

Figure 5. A) Resonance Raman spectra of complex **2** containing a) ^{16}O and b) ^{18}O. c) Difference spectrum of (a)−(b); B) Resonance Raman spectra of [(tmpIm)Fe^{III}–OOD] containing a) ^{16}O and b) ^{18}O. c) Difference spectrum of (a)−(b). $\lambda_{ex} = 429.6$ nm, 77 K.

These UV/Vis spectral features are similar to those of complex **2**. The EPR spectrum of this species has the same set of g values ($g = 2.32$, 2.19, 1.95) as complex **2** (Figure 4, inset). Thus, these results indicate that the same compound was prepared by the two different routes. Complex **2** was further characterized by rR spectroscopy. The rR spectra reveal isotope shifts of 810(^{16}O)/763(^{18}O) cm^{-1} in the region near 800 cm^{-1} and of 570(^{16}O)/544(^{18}O) cm^{-1} in the low-frequency region (Figure 5A). Deuterium substitution of complex **2** with MeOD produced a 4 cm^{-1} upshift of the ν(O–O) band and a 4 cm^{-1} downshift of the ν(Fe–O) band (Figure 5B). These H/D substitution shifts are in good agreement with previously reported rR data for metallo–hydroperoxo species and are consistent with the existence of hydrogen-bonding between the hydroperoxo and methanol molecules.[16] Thus, the modes at 810 and 570 cm^{-1} can be assigned to the hydroperoxide ν(O–O) and ν(Fe–O) stretching vibrations, respectively. The observed ν(O–O) and ν(Fe–O) values are comparable to those of the hydroperoxo intermediate isolated by the cryoreduction method with cytochrome P450 whose ν(O–O) and ν(Fe–O) modes appear at 774 and 564 cm^{-1}, respectively.[16a]

The characterization of complex **2** was further corroborated by Mössbauer data. The zero-field Mössbauer spectra of ^{57}Fe-enriched complexes **2** was measured at 80 K. The Mössbauer spectrum of complex **2** exhibits a quadrupole doublet characterized by an isomer shift δ_{Fe} of 0.25 $mm\,s^{-1}$ and a quadrupole splitting ΔE_q of 2.16 $mm\,s^{-1}$. These parameters are typical for a low-spin ferric species and are in agreement with those of the hydroperoxo–heme species ($\delta_{Fe} = 0.29$ $mm\,s^{-1}$, $\Delta E_q = 2.03$ $mm\,s^{-1}$) from heme oxygenase.[7d]

It is worth noting that complex **2** may also be generated through a one-electron reduction of the oxy form [(tmpIm)$Fe^{III}(O_2^-)$] in the presence of a proton source. This reaction occurs in a similar manner to that of the catalytic processes of heme enzyme systems. Oxygenation of a solution of [(tmpIm)Fe^{II}] in EtCN/THF (20:80) in the presence of methanol (400 equiv) at −75 °C produced the corresponding dioxygen adduct, which represents a superoxide species [(tmpIm)$Fe^{III}(O_2^-)$] and has UV/Vis absorption maxima at 426, 535, and 589 nm. After removal of the excess dioxygen, addition of one equivalent of cobaltocene ([$CoCp_2$]) immediately produces a new species with UV/Vis absorption maxima at $\lambda_{max} = 427$, 534, 564 and 610 nm. These features

are similar to those of complex **2** obtained in the reaction of [(tmpIm)Fe^{II}] with KO_2 in the presence of methanol in the same solvents (Figure 6). The EPR spectrum of this species shows signals at $g = 2.32$, 2.19, and 1.95, which confirm its identification as complex **2** (Figure 6, inset). As expected, the

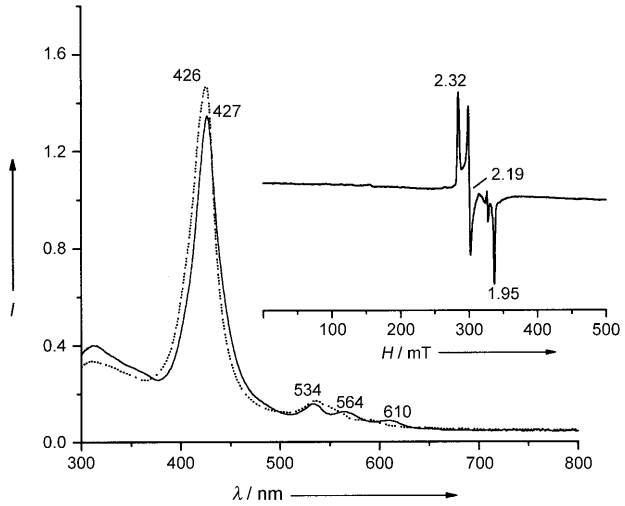

Figure 6. UV/Vis spectra of ferric superoxide [(tmpIm)$Fe^{III}(O_2^-)$] (••••) and its [$CoCp_2$] reduction products in the presence of 400 equiv of methanol (complex **2**, ——) in EtCN/THF (20:80) at −75 °C. The inset shows the EPR spectrum of complex **2** as prepared above.

hydroperoxo compound [(tmpIm)Fe^{III}–OOH] can therefore be prepared by using the methods outlined above (Scheme 1).

In summary, efficient methods for preparation of low-spin end-on ferric hydroperoxo heme species from an imidazole-tailed porphyrin [(tmpIm)Fe^{II}] have been demonstrated. We have shown for the first time that protonation of a 7c side-on heme peroxide can switch its spin state from high- to low-spin and convert the η^2 binding mode to a monodentate configuration. Furthermore, we succeeded in mimicking the proton-coupled electron-transfer (PCET) formation of a hydroperoxo heme species in a manner similar to that occurring in the catalytic processes of enzyme systems. The experimental results suggest that the axial imidazole ligation to the heme is crucial for O_2 activation, which occurs through the formation of a metastable hydroperoxo species. This model complex will provide a convenient system for exploring the nature of unstable hydroperoxo reactive intermediates that are difficult to observe under ambient catalytic turnover of the enzymes. Results thus obtained will provide a benchmark for characterization and assignment of important hydroperoxo–heme intermediates.

Received: August 17, 2009
Published online: October 30, 2009

Keywords: bioinorganic chemistry · enzyme models · heme proteins · iron · O–O activation

[1] D. J. Stuehr, *Biochim. Biophys. Acta Bioenerg.* **1999**, *1411*, 217–230.
[2] a) I. G. Denisov, T. M. Makris, S. G. Sligar, I. Schlichting, *Chem. Rev.* **2005**, *105*, 2253; b) S. Jin, A. Bryson, J. H. Dawson, *J. Biol. Inorg. Chem.* **2004**, *9*, 644–653.
[3] M. Unno, T. Mastui, M. Ikeda-Saito, *Nat. Prod. Rep.* **2007**, *24*, 553–570.
[4] a) K. Kuhnel, E. Derat, J. Terner, S. Shaik, I. Schlichting, *Proc. Natl. Acad. Sci. USA* **2007**, *104*, 99–104; b) I. G. Denisov, J. H. Dawson, L. P. Hager, S. G. Sligar, *Biochem. Biophys. Res. Commun.* **2007**, *363*, 954–958; c) I. G. Denisov, T. M. Makris, S. G. Sligar, *J. Biol. Chem.* **2002**, *277*, 42706–42710.
[5] E. Kim, E. E. Chufan, K. Kamaraj, K. D. Karlin, *Chem. Rev.* **2004**, *104*, 561–588.
[6] a) M. C. R. Symons, R. L. Petersen, *Biochim. Biophys. Acta Protein Struct.* **1978**, *537*, 70–76; b) R. Kappl, M. Hoehn-Berlage, J. Huettermann, N. Bartlett, M. C. R. Symons, *Biochim. Biophys. Acta Protein Struct. Mol. Enzymol.* **1985**, *827*, 327–343.
[7] a) W. Leibl, W. Nitschke, J. Huttermann, *Biochim. Biophys. Acta Protein Struct. Mol. Enzymol.* **1986**, *870*, 20–30; b) R. Davydov, J. D. Satterlee, H. Fujii, A. Sauer-Masarwa, D. H. Busch, B. M. Hoffman, *J. Am. Chem. Soc.* **2003**, *125*, 16340–16346; c) M. Ibrahim, I. G. Denisov, T. M. Makris, J. R. Kincaid, S. G. Sligar, *J. Am. Chem. Soc.* **2003**, *125*, 13714–13718; d) R. Garcia-Serres, R. Davydov, T. Matsui, M. Ikeda-Saito, B. M. Hoffman, B. H. Huynh, *J. Am. Chem. Soc.* **2007**, *129*, 1402–1412; e) M. Unno, H. Chen, S. Kusama, S. Shaik, M. Ikeda-Saito, *J. Am. Chem. Soc.* **2007**, *129*, 13394–13395.
[8] a) R. Davydov, A. Ledbetter-Rogers, P. Martasek, M. Larukhin, M. Sono, J. H. Dawson, B. S. S. Masters, B. M. Hoffman, *Biochemistry* **2002**, *41*, 10375–10381; b) R. Davydov, R. Perera, S. Jin, T.-C. Yang, T. A. Bryson, M. Sono, J. H. Dawson, B. M. Hoffman, *J. Am. Chem. Soc.* **2005**, *127*, 1403–1413.
[9] a) R. Davydov, T. Yoshida, M. Ikeda-Saito, B. M. Hoffman, *J. Am. Chem. Soc.* **1999**, *121*, 10656–10657; b) R. Davydov, V. Kofman, H. Fujii, T. Yoshida, M. Ikeda-Saito, B. M. Hoffman, *J. Am. Chem. Soc.* **2002**, *124*, 1798–1808.
[10] a) J. D. Soper, S. V. Kryatov, E. V. Rybak-Akimova, D. G. Nocera, *J. Am. Chem. Soc.* **2007**, *129*, 5069–5075; b) N. Suzuki, T. Higuchi, T. Nagano, *J. Am. Chem. Soc.* **2002**, *124*, 9622–9628; c) Y. Watanabe, *J. Biol. Inorg. Chem.* **2001**, *6*, 846–856; d) E. Kim, K. Kamaraj, B. Galliker, N. D. Rubie, P. Moenne-Loccoz, S. Kaderli, A. D. Zuberbuhler, K. D. Karlin, *Inorg. Chem.* **2005**, *44*, 1238–1247.
[11] a) K. Dürr, B. P. Macpherson, R. Warratz, F. Hampel, T. Tuczek, M. Helmreich, N. Jux, I. Ivanovic-Burmazovic, *J. Am. Chem. Soc.* **2007**, *129*, 4217–4228; b) E. E. Chufán, K. D. Karlin, *J. Am. Chem. Soc.* **2003**, *125*, 16160–16161; c) D. Mandon, R. Weiss, M. Franke, E. Bill, A. X. Trautwein, *Angew. Chem.* **1989**, *101*, 1747–1750; *Angew. Chem. Int. Ed. Engl.* **1989**, *28*, 1709–1711.
[12] a) J. Annaraj, J. Cho, Y.-M. Lee, S. Y. Kim, R. Latifi, S. P. de Visser, W. Nam, *Angew. Chem.* **2009**, *121*, 4214–4217; *Angew. Chem. Int. Ed.* **2009**, *48*, 4150–4153; b) W. Nam, *Acc. Chem. Res.* **2007**, *40*, 522–531; c) D. L. Wertz, J. S. Valentine, *Struct. Bonding (Berlin)* **2000**, *97*, 37–60, and references therein; d) M. Selke, J. S. Valentine, *J. Am. Chem. Soc.* **1998**, *120*, 2652–2653; e) J. N. Burstyn, J. A. Roe, A. R. Miksztal, B. A. Shaevitz, G. Lang, J. S. Valentine, *J. Am. Chem. Soc.* **1988**, *110*, 1382–1388; f) E. McCandlish, A. R. Miksztal, M. Nappa, A. Q. Sprenger, J. S. Valentine, J. D. Stong, T. G. Spiro, *J. Am. Chem. Soc.* **1980**, *102*, 4268–4271. In this paper, preliminary rR characterization of the side-on heme-peroxide [(dmso)(oep)$Fe(O_2^{2-})$] (oep = octaethylporphyrin) was attempted, however, the band at 780 cm^{-1}, which was tentatively assigned to ν(O–O), was significant lower than that of the corresponding IR band (806 cm^{-1}).

[13] a) K. Tajima, S. Oka, T. Edo, S. Miyake, H. Mano, K. Mukai, H. Sakurai, K. Ishizu, *J. Chem. Soc. Chem. Commun.* **1995**, 1507 – 1508; b) K. Tajima, M. Shigematsu, J. Jinno, K. Ishizu, H. Ohya-Nishihuchi, *J. Chem. Soc. Chem. Commun.* **1990**, 144 – 145; c) K. Tajima, J. Jinno, K. Ishizu, H. Sakurai, H. Ohya-Nishiguchi, *Inorg. Chem.* **1989**, *28*, 709 – 715; d) M. Rivera, G. A. Caignan, A. V. Astashkin, A. M. Raitsimring, T. K. Shokhireva, F. A. Walker, *J. Am. Chem. Soc.* **2002**, *124*, 6077 – 6089.

[14] a) J.-G. Liu, Y. Naruta, F. Tani, *Angew. Chem.* **2005**, *117*, 1870 – 1874; *Angew. Chem. Int. Ed.* **2005**, *44*, 1836 – 1840; b) J.-G. Liu, Y. Naruta, F. Tani, T. Chishiro, Y. Tachi, *Chem. Commun.* **2004**, 120 – 121; c) J.-G. Liu, Y. Naruta, F. Tani, *Chem. Eur. J.* **2007**, *13*, 6365 – 6378; d) T. Chishiro, Y. Shimazaki, F. Tani, Y. Tachi, Y. Naruta, S. Karasawa, S. Hayami, Y. Maeda, *Angew. Chem.* **2003**, *115*, 2894 – 2897; *Angew. Chem. Int. Ed.* **2003**, *42*, 2788 – 2791.

[15] a) A. J. Simaan, S. Dopner, F. Banse, S. Bourcier, G. Bouchoux, A. Boussac, P. Hildebrandt, J.-J. Girerd, *Eur. J. Inorg. Chem.* **2000**, 1627 – 1633; b) G. Roelfes, V. Vrajmasu, K. Chen, R. Y. N. Ho, J.-U. Rohde, C. Zondervan, R. M. Crois, E. P. Schudde, M. Lutz, A. L. Spek, R. Hage, B. L. Feringa, E. Münck, L. Que, Jr., *Inorg. Chem.* **2003**, *42*, 2639 – 2653; c) F. Neese, E. I. Solomon, *J. Am. Chem. Soc.* **1998**, *120*, 12829 – 12848.

[16] a) I. G. Denisov, P. J. Mak, T. M. Makris, S. G. Sligar, J. R. Kinkaid, *J. Phys. Chem. A* **2008**, *112*, 13172 – 13179; b) P. J. Mak, I. G. Denisov, D. Victoria, T. M. Makris, T. Deng, S. G. Sligar, J. R. Kincaid, *J. Am. Chem. Soc.* **2007**, *129*, 6382 – 6383; c) M. Ibrahim, I. G. Denisov, T. M. Makris, J. R. Kincaid, S. G. Sligar, *J. Am. Chem. Soc.* **2003**, *125*, 13714 – 13718; d) T. Kitagawa, M. R. Ondrias, D. L. Rousseau, M. Ikeda-Saito, T. Yonetani, *Nature* **1982**, *298*, 869 – 871.

